

Quasinormal modes and absorption probabilities of spin-3/2 fields in D -dimensional Reissner-Nordström black hole spacetimes

C.-H. Chen,^{1,*} H. T. Cho,^{2,†} A. S. Cornell,^{3,‡} G. Harmsen,^{3,§} and X. Ngcobo^{3,||}

¹*Institute of Physics, Academia Sinica, Nankang, Taipei 11529, Taiwan*

²*Department of Physics, Tamkang University, Tamsui District, New Taipei City 25137, Taiwan*

³*National Institute for Theoretical Physics; School of Physics, University of the Witwatersrand, Wits 2050, Johannesburg, South Africa*



(Received 3 November 2017; published 25 January 2018)

In this paper we consider spin-3/2 fields in a D -dimensional Reissner-Nordström black hole spacetime. As these spacetimes are not Ricci flat, it is necessary to modify the covariant derivative to the supercovariant derivative, by including terms related to the background electromagnetic fields, so as to maintain the gauge symmetry. Using this supercovariant derivative we arrive at the corresponding Rarita-Schwinger equation in a charged black hole background. As in our previous works, we exploit the spherical symmetry of the spacetime and use the eigenspinor vectors on an N sphere to derive the radial equations for both nontransverse-traceless (non-TT) modes and TT modes. We then determine the quasinormal mode and absorption probabilities of the associated gauge-invariant variables using the WKB approximation and the asymptotic iteration method. We then concentrate on how these quantities change with the charge of the black hole, especially when they reach the extremal limits.

DOI: [10.1103/PhysRevD.97.024038](https://doi.org/10.1103/PhysRevD.97.024038)

I. INTRODUCTION

In supergravity theories [1,2] the gravitino is described by a spin-3/2 field. The equations of motion of these spin-3/2 fields are given by the Rarita-Schwinger equation,

$$\gamma^{\mu\nu\alpha}\nabla_\nu\psi_\alpha = 0, \quad (1.1)$$

where

$$\gamma^{\mu\nu\alpha} \equiv \gamma^{[\mu}\gamma^\nu\gamma^{\alpha]} = \gamma^\mu\gamma^\nu\gamma^\alpha - \gamma^\mu g^{\nu\alpha} + \gamma^\nu g^{\mu\alpha} - \gamma^\alpha g^{\mu\nu} \quad (1.2)$$

is the antisymmetric product of Dirac gamma matrices, ∇_ν is the covariant derivative, and ψ_α is the spin-3/2 field. In four-dimensional black hole spacetimes the Rarita-Schwinger equations are usually analyzed in the Newman-Penrose formalism. However, this formalism cannot be extended to higher dimensions in a straightforward way. In our previous works [3,4] we have tried an alternative approach to deal with spherically symmetric black hole cases. Using a complete set of eigenspinor vectors on N spheres, we were able to separate the radial and angular parts of the Rarita-Schwinger equation. In this paper

we extend our considerations to charged black hole spacetimes.

The Rarita-Schwinger equation is invariant under the gauge transformation

$$\psi'_\alpha = \psi_\alpha + \nabla_\alpha\varphi, \quad (1.3)$$

where φ is a gauge spinor, provided that the background spacetime is Ricci flat [3,4]. This is not the case for charged black holes, nor for black holes in de Sitter or anti-de Sitter spaces. To maintain the gauge symmetry in those cases it is necessary to modify the covariant derivative into the so-called “supercovariant derivative.” This is done by adding terms related to the cosmological constant and the electromagnetic field of the black hole. Here we concentrate on charged Reissner-Nordström black holes in asymptotically flat spacetimes, where in the following section we show in detail how the supercovariant derivative is constructed in this case.

Using the supercovariant derivative we are able to obtain the Rarita-Schwinger equation for spin-3/2 fields in Reissner-Nordström black hole spacetimes. Since the spacetime is still spherically symmetric, it is possible, as in our previous works, to derive the radial equations for each component of the spin-3/2 field using eigenspinor vectors on the N sphere. However, the component fields are not gauge invariant, while the physical fields should be. Hence we, as in Ref. [4], construct a combination of the component fields, which is gauge invariant. That is, we use the

*chunhungchen928@gmail.com

†htcho@mail.tku.edu.tw

‡alan.cornell@wits.ac.za

§gerhard.harmsen5@gmail.com

||540630@students.wits.ac.za

same gauge-invariant variables and work out the corresponding radial equations.

As the aim in this paper is to study spin-3/2 fields near a Reissner-Nordström black hole, we focus on how the charge Q of the black hole affects the behavior of the fields. This is done by studying the quasinormal models (QNMs) associated to our fields, where QNMs are characterized by their complex frequencies. The real parts of the frequencies represent the frequencies of oscillations, while the imaginary parts represent the decay constants of damping. These QNMs are uniquely determined by the parameters of the black hole [5], where in order to determine these QNMs we use the WKB and improved asymptotic iterative method (AIM), where these methods and how to implement them are given in Refs. [4,6,7]. Finally, using the WKB method we are able to obtain the absorption probabilities associated to our spin-3/2 fields, which can give us an insight into the grey-body factors and cross sections of the black hole.

As such, this paper is set out as follows: In the next section we give a brief motivation for the form of our supercovariant derivative, and in Sec. III we use this supercovariant derivative to determine our equations of motion, and the potential functions for both the non-TT and the TT eigenmodes of our fields. In Sec. IV, we present the QNMs for our spin-3/2 fields near the Reissner-Nordström black hole. The corresponding absorption probabilities are laid out in Sec. V. Finally, in Sec. VI, we give concluding remarks on our results.

II. SUPERCOVARIANT DERIVATIVE

In order to ensure that our Rarita-Schwinger equation, $\gamma^{\mu\nu\alpha}\nabla_\nu\psi_\alpha=0$, remains true, we must require that our spinor vectors, ψ_μ , are invariant under the transformation in Eq. (1.3). This is guaranteed if

$$\frac{1}{2}\gamma^{\mu\nu\alpha}[\nabla_\nu, \nabla_\alpha]\varphi=0, \quad (2.1)$$

which is satisfied when the metric is a Ricci flat spacetime [4]. However, in the case of the Reissner-Nordström metric this is not necessarily true, and so we must first determine the supercovariant derivative, $\tilde{\mathcal{D}}_\mu$. We make the assumption that the derivative has the form

$$\tilde{\mathcal{D}}_\mu = \mathcal{D}_\mu + b\gamma^\rho F_{\mu\rho} + c\gamma_{\mu\rho\sigma}F^{\rho\sigma}, \quad (2.2)$$

which needs to satisfy

$$\frac{1}{2}\gamma^{\lambda\mu\nu}[\tilde{\mathcal{D}}_\mu, \tilde{\mathcal{D}}_\nu]\varphi=0, \quad (2.3)$$

where $\mathcal{D}_\mu = \nabla_\mu - ieA_\mu$, $F_{\mu\nu}$ is the electromagnetic field, and b, c are unknown constants. Plugging Eq. (2.2) into Eq. (2.3) we have

$$\begin{aligned} 0 = & 4c(D-2)(\nabla_\mu F^{\mu\lambda})\varphi + \gamma^\mu[G_\mu{}^\lambda - 4(b^2 + 2c(D-3))F_{\mu\nu}F^{\nu\lambda} - 2(b^2 - 2c^2(D-3)(D-4))g_\mu{}^\lambda F_{\rho\sigma}F^{\rho\sigma}]\varphi \\ & + \gamma^{\mu\nu}[(b + 2c(D-3))(2g_\mu{}^\lambda \nabla_\alpha F^\alpha{}_\nu - \nabla^\lambda F_{\mu\nu})]\varphi + \gamma^{\mu\rho\sigma}[-ieg_\mu{}^\lambda F_{\rho\sigma} + 4(b + 2c(D-3))(b + c(D-6))F_{\rho\sigma}F_\mu{}^\lambda]\varphi \\ & + \gamma^{\lambda\mu\nu\rho\sigma}[-2(b^2 + 2bc(D-5) + c^2(D^2 - 11D + 26))]F_{\mu\nu}F_{\rho\sigma}\varphi. \end{aligned} \quad (2.4)$$

Setting $\gamma^{\mu\nu}$ equal to 0 we have $b = -2(D-3)c$, and together with Eq. (2.4) we have

$$\begin{aligned} 0 = & 4c(D-2)(\nabla_\mu F^{\mu\lambda})\varphi + \gamma^\mu \left[G_\mu{}^\lambda + 16(D-2)(D-3)c^2 \left(F_{\mu\nu}F^{\lambda\nu} - \frac{1}{4}g_\mu{}^\lambda F_{\rho\sigma}F^{\rho\sigma} \right) \right] \varphi \\ & + \gamma^{\mu\rho\sigma}[-ieg_\mu{}^\lambda F_{\rho\sigma}] + \gamma^{\lambda\mu\nu\rho\sigma}(-2c^2)(D-1)(D-2)F_{\mu\nu}F_{\rho\sigma}\varphi. \end{aligned} \quad (2.5)$$

In order to remove the γ^μ terms we require that

$$G_\mu{}^\lambda + 16(D-2)(D-3)c^2 \left(F_{\mu\nu}F^{\lambda\nu} - \frac{1}{4}g_\mu{}^\lambda F_{\rho\sigma}F^{\rho\sigma} \right) = 0, \quad (2.6)$$

where

$$16(D-2)(D-3)c^2 = -\frac{1}{2} \Rightarrow c = \frac{i}{4\sqrt{2(D-2)(D-3)}}, \quad (2.7)$$

and with the $\gamma^{\mu\rho\sigma}$ term equal to 0 only when $e = 0$. Next we consider the γ^μ and $\gamma^{\lambda\mu\nu\rho\sigma}$ terms. In the four-dimensional case, $\gamma^{\lambda\mu\nu\rho\sigma} = 0$ and $\nabla_\mu F^{\mu\lambda} = 0$, which is the Maxwell equation, and Eq. (2.5) is automatically satisfied. In the five-dimensional case, $\gamma^{\lambda\mu\nu\rho\sigma}$ is proportional to the identity matrix, such that we have to set the equations of motion for the electromagnetic field (where $D = 5$) as

$$\nabla_\mu F^{\mu\lambda} = -\frac{1}{4\sqrt{3}}\epsilon^{\lambda\mu\nu\rho\sigma}F_{\mu\nu}F_{\rho\sigma}, \quad \epsilon^{tr\theta_1\theta_2\theta_3} = \frac{1}{\sqrt{-g}}, \quad (2.8)$$

where $\epsilon^{\lambda\mu\nu\rho\sigma}$ is the Levi-Civita tensor. In higher dimensional cases we can take the equations of motion for

electromagnetic field to be $\nabla_\mu F^{\mu\lambda} = 0$, and the $\gamma^{\lambda\mu\nu\rho\sigma}$ term vanishes if the condition $F_{[\mu\nu}F_{\rho\sigma]} = 0$ is fulfilled. Finally the supercovariant derivative for the spin-3/2 field in a general dimensional Reissner-Nordström black hole space-time can be written as

$$\tilde{\mathcal{D}}_\mu = \nabla_\mu + \frac{1}{2} \sqrt{\frac{D-3}{2(D-2)}} \gamma_\rho F_\mu{}^\rho + \frac{i}{4\sqrt{2(D-2)(D-3)}} \gamma_{\mu\rho\sigma} F^{\rho\sigma}. \quad (2.9)$$

Note that this is consistent with the results of Ref. [8], though we must emphasize that in our construction one cannot find an appropriate supercovariant derivative for a “charged” spin-3/2 field in the Reissner-Nordström black hole spacetime.

III. POTENTIAL FUNCTION

In this section we determine both the radial equations and the potential functions for our spin-3/2 fields near the Reissner-Nordström black hole, using the same approach as we have done for the N -dimensional Schwarzschild black hole. For completeness we reproduce some of the results from the Schwarzschild case in this paper, where a full explanation of this method can be found in Ref. [4].

A. Rarita-Schwinger field near D-dimensional Reissner-Nordström black holes

Our line element is given as [8]

$$ds^2 = -f dt^2 + \frac{1}{f} dr^2 + r^2 d\bar{\Omega}_N^2, \quad (3.1)$$

where $f = 1 - \frac{2M}{r^{D-3}} + \frac{Q^2}{r^{(2D-6)}}$ and $D = N + 2$. The term $d\bar{\Omega}_N$ denotes the metric of the N sphere S^N , where we use over bars to represent terms from this metric. Next, the electromagnetic field takes the Coulomb form which is given as [9]

$$F_{tr} = \frac{q}{r^{(D-2)}}, \quad A_t = \frac{q}{(D-3)r^{(D-3)}}. \quad (3.2)$$

The relation of Q and q is

$$Q^2 = \frac{\kappa^2 q^2}{(D-2)(D-3)}, \quad (3.3)$$

where κ^2 is a constant defined by the Einstein field equation,

$$G_{\mu\nu} = \kappa^2 \left(F_{\mu\lambda} F_\nu{}^\lambda - \frac{1}{4} g_{\mu\nu} F_{\rho\sigma} F^{\rho\sigma} \right). \quad (3.4)$$

In order to be consistent with the supercovariant derivative above, one should take $\kappa^2 = 1/2$ as in Eq. (2.7). Since we represent the wave functions of our fields as spinor vectors, which can be constructed from the non-TT eigemodes and the TT eigenmodes on S^N , we use the massless form of the Rarita-Schwinger equation [4],

$$\gamma^{\mu\alpha} \tilde{\mathcal{D}}_\nu \psi_\alpha = 0, \quad (3.5)$$

where $\tilde{\mathcal{D}}_\nu$ is the supercovariant derivative in Eq. (2.9).

B. Non-TT eigenfunctions

The radial and temporal wave functions can be written as

$$\psi_r = \phi_r \otimes \bar{\psi}_{(\lambda)} \quad \text{and} \quad \psi_t = \phi_t \otimes \bar{\psi}_{(\lambda)}, \quad (3.6)$$

where $\bar{\psi}_{(\lambda)}$ is an eigenspinor on S^N , with eigenvalue $i\bar{\lambda}$. The eigenvalues $\bar{\lambda}$ are given by $\bar{\lambda} = (j + (D-3)/2)$, where $j = 3/2, 5/2, 7/2, \dots$ [4]. Our angular wave function is written as

$$\psi_{\theta_i} = \phi_\theta^{(1)} \otimes \bar{\nabla}_{\theta_i} \bar{\psi}_{(\lambda)} + \phi_\theta^{(2)} \otimes \bar{\gamma}_{\theta_i} \bar{\psi}_{(\lambda)}, \quad (3.7)$$

where $\phi_\theta^{(1)}, \phi_\theta^{(2)}$ are functions of r and t which behave like 2-spinors. We begin by using the Weyl gauge, $\phi_t = 0$, and then introduce a gauge-invariant variable, which we also use to determine the equations of motion. Looking at $\mu = r$, $\mu = t$ and $\mu = \theta$ equations in Eq. (3.5) separately, we determine the four appropriate equations of motion. Note that our choice of the gamma tensors and the spin connections can be found in Ref. [4].

1. Equations of motion

First consider the case of $\mu = t$ in Eq. (3.5),

$$\gamma^{\nu\alpha} \tilde{\mathcal{D}}_\nu \psi_\alpha = 0. \quad (3.8)$$

Using the definitions of our wave functions we determine our first equation of motion to be

$$\begin{aligned} 0 = & - \left(i\bar{\lambda} + (D-2) \frac{\sqrt{f}}{2} i\sigma^3 + (D-2) \frac{iQ}{2r^{D-3}} \right) \phi_r \\ & + \left(i\bar{\lambda} \partial_r - \frac{1}{4} \frac{(D-2)(D-3)}{r\sqrt{f}} i\sigma^3 + (D-3) \frac{i\bar{\lambda}}{2r} \right) \phi_\theta^{(1)} \\ & + \left((D-2) \partial_r + (D-3) \frac{i\bar{\lambda}}{r\sqrt{f}} i\sigma^3 + \frac{(D-2)(D-3)}{2r} \right) \phi_\theta^{(2)}. \end{aligned} \quad (3.9)$$

Next we consider $\mu = r$, and get the second equation of motion as

$$0 = \left[-\frac{i\bar{\lambda}}{\sqrt{f}}\partial_t + \frac{i\bar{\lambda}f'}{4\sqrt{f}}\sigma^1 - \frac{(D-3)(D-2)}{4r}\sigma^2 + (D-3)\frac{i\bar{\lambda}\sqrt{f}}{2r}\sigma^1 \right] \phi_\theta^{(1)} \\ + \left[-\frac{D-2}{\sqrt{f}}\partial_t + \frac{(D-2)f'}{4\sqrt{f}}\sigma^1 + (D-3)\frac{i\bar{\lambda}}{r}\sigma^2 + (D-2)(D-3)\frac{\sqrt{f}}{2r}\sigma^1 \right] \phi_\theta^{(2)}. \quad (3.10)$$

Finally for the case of $\mu = \theta_i$ we obtain two more equations,

$$0 = \left(\partial_t - \frac{f'}{4}\sigma^1 + i\bar{\lambda}\frac{\sqrt{f}}{r}\sigma^2 - (D-3)\frac{f}{2r}\sigma^1 \right) \phi_r + \left(\frac{\bar{\lambda}}{r\sqrt{f}}\sigma^3\partial_t - i\bar{\lambda}\frac{f'}{4r\sqrt{f}}\sigma^2 - i\bar{\lambda}\frac{\sqrt{f}}{r}\sigma^2\partial_r - \frac{(D-3)(D-4)}{4r^2}\sigma^1 \right. \\ \left. - i\bar{\lambda}(D-4)\frac{\sqrt{f}}{2r^2}\sigma^2 - \bar{\lambda}(D-2)\frac{Q}{2r^{D-1}}\sigma^1 \right) \phi_\theta^{(1)} + \left(-\frac{D-3}{r\sqrt{f}}i\sigma^3\partial_t - (D-3)\frac{f'}{4r\sqrt{f}}\sigma^2 - (D-3)\frac{\sqrt{f}}{r}\sigma^2\partial_r \right. \\ \left. + (D-4)\frac{i\bar{\lambda}}{r^2}\sigma^1 - (D-3)(D-4)\frac{\sqrt{f}}{2r^2}\sigma^2 + (D-3)(D-2)\frac{iQ}{2r^{D-1}}\sigma^1 \right) \phi_\theta^{(2)} \quad (3.11)$$

$$0 = -\frac{\sqrt{f}}{r}\sigma^2\phi_r + \left(\frac{1}{r\sqrt{f}}i\sigma^3\partial_t + \frac{f'}{4r\sqrt{f}}\sigma^2 + \frac{\sqrt{f}}{r}\sigma^2\partial_r + (D-4)\frac{\sqrt{f}}{2r^2}\sigma^2 - (D-2)\frac{iQ}{2r^{D-1}}\sigma^1 \right) \phi_\theta^{(1)} - \frac{D-4}{r^2}\sigma^1\phi_\theta^{(2)}. \quad (3.12)$$

It can be shown that these four equations of motion are not independent. One of them can be obtained from the other three. Hence we work with only Eqs. (3.9), (3.10) and (3.12) in the following.

2. Effective potential

The functions ϕ_r , $\phi_\theta^{(1)}$ and $\phi_\theta^{(2)}$ are not gauge invariant, and as such we apply a gauge-invariant variable to our equations of motion. Using the same arguments as we have used in Ref. [4] we obtain the following gauge-invariant variable:

$$\Phi = -\left(\frac{\sqrt{f}}{2}i\sigma^3 + \frac{iQ}{2r^{D-3}} \right) \phi_\theta^{(1)} + \phi_\theta^{(2)}. \quad (3.13)$$

Plugging this into Eqs. (3.9), (3.10) and (3.12) we obtain the equation of motion for the gauge-invariant variable Φ ,

$$\left((D-2)\frac{\sqrt{f}}{2} + \left(\bar{\lambda} + (D-2)\frac{Q}{2r^{D-3}} \right) \sigma^3 \right) \left[-\frac{D-2}{f}\sigma^1\partial_t + (D-2)\frac{f'}{4f} - \frac{(D-3)\bar{\lambda}}{r\sqrt{f}}\sigma^3 + \frac{(D-2)(D-3)}{2r} \right] \Phi \\ = \left((D-2)\frac{\sqrt{f}}{2} - \left(\bar{\lambda} + (D-2)\frac{Q}{2r^{D-3}} \right) \sigma^3 \right) \left[(D-2)\partial_r - \frac{\bar{\lambda}}{r\sqrt{f}}\sigma^3 + \frac{(2D-7)(D-2)}{2r} + (D-2)(D-4)\frac{Q}{2r^{D-2}\sqrt{f}}\sigma^3 \right] \Phi. \quad (3.14)$$

Componentwise, Φ can be written as

$$\Phi = \begin{pmatrix} \phi_1 e^{-i\omega t} \\ \phi_2 e^{-i\omega t} \end{pmatrix}, \quad (3.15)$$

where ϕ_1 and ϕ_2 are purely radially dependent terms. Furthermore we set

$$\phi_1 = \frac{(\frac{D-2}{2})^2 f - (\bar{\lambda} + C)^2}{Br^{\frac{D-4}{2}} f^{1/4}} \tilde{\phi}_1 \quad \text{and} \\ \phi_2 = \frac{(\frac{D-2}{2})^2 f - (\bar{\lambda} - C)^2}{Ar^{\frac{D-4}{2}} f^{1/4}} \tilde{\phi}_2, \quad (3.16)$$

where

$$A = \frac{D-2}{2}\sqrt{f} + (\bar{\lambda} + C), \quad B = \frac{D-2}{2}\sqrt{f} - (\bar{\lambda} + C) \\ \text{and } C = (D-2)\frac{Q}{2r^{D-3}}. \quad (3.17)$$

Applying Eqs. (3.15) and (3.16) to Eq. (3.14) we get the following set of coupled equations:

$$(f\partial_r - W)\tilde{\phi}_1 = i\omega\tilde{\phi}_2, \quad (f\partial_r + W)\tilde{\phi}_2 = i\omega\tilde{\phi}_1, \quad (3.18)$$

where

$$W = \frac{(D-3)\sqrt{f}}{rAB} \left[(\bar{\lambda} + C) \frac{2}{D-2} AB + \frac{D-2}{2} (C + \bar{\lambda}(1-f)) \right] - \frac{D-4}{r(D-2)} \sqrt{f}(\bar{\lambda} + C). \quad (3.19)$$

Decoupling these two equations we obtain the following radial equations,

$$-\frac{d^2}{dr_*^2} \tilde{\phi}_1 + V_1 \tilde{\phi}_1 = \omega^2 \tilde{\phi}_1, \quad -\frac{d^2}{dr_*^2} \tilde{\phi}_2 + V_2 \tilde{\phi}_2 = \omega^2 \tilde{\phi}_2, \quad (3.20)$$

where r_* is the tortoise coordinate with the definition $dr_* = \frac{1}{f(r)} dr$, and

$$V_{1,2} = \pm f(r) \frac{dW}{dr} + W^2.$$

Setting $Q = 0$ in Eq. (3.20) we recover the Schwarzschild potential as given in Ref. [4].

C. TT eigenfunctions

1. Equations of motion

Setting the ψ_r and ψ_t to be the same as in the non-TT eigenfunctions case given in Eq. (3.6), the angular part is now given as

$$\psi_{\theta_i} = \phi_\theta \otimes \tilde{\psi}_{\theta_i}, \quad (3.21)$$

where $\tilde{\psi}_{\theta_i}$ is the TT mode eigenspinor vector which includes the “TT mode I” and “TT mode II,” as described in Ref. [4], and ϕ_θ behaves like a 2-spinor. We again initially use the Weyl gauge, and in this case apply the TT conditions on a sphere, giving us $\phi_t = \phi_r = 0$ [4]. Our only nonzero equation of motion is then determined to be

$$\left(\frac{1}{r\sqrt{f}} i\sigma^3 \partial_t + \frac{\sqrt{f}}{r} \sigma^2 \partial_r + \frac{f'}{4r\sqrt{f}} \sigma^2 + (D-4) \frac{\sqrt{f}}{2r^2} \sigma^2 + \frac{i\bar{\zeta}}{r^2} \sigma^1 - (D-2) \frac{iQ}{2r^{D-1}} \sigma^1 \right) \phi_\theta = 0, \quad (3.22)$$

where in this case ϕ_θ is already gauge invariant. We can therefore use this equation to determine our radial equation.

2. Effective potential

We can rewrite ϕ_θ as

$$\phi_\theta = \sigma^2 \begin{pmatrix} \Psi_{\theta_1} e^{-i\omega t} \\ \Psi_{\theta_2} e^{-i\omega t} \end{pmatrix}, \quad (3.23)$$

and substituting Eq. (3.23) into Eq. (3.22) we get the following set of coupled equations:

$$\begin{aligned} \left(f\partial_r + \frac{f'}{4} + (D-4) \frac{f}{2r} - \left(\frac{\bar{\zeta}\sqrt{f}}{r} - (D-2) \frac{Q\sqrt{f}}{2r^{D-2}} \right) \right) \Psi_{\theta_1} &= i\omega \Psi_{\theta_2}, \\ \left(f\partial_r + \frac{f'}{4} + (D-4) \frac{f}{2r} + \left(\frac{\bar{\zeta}\sqrt{f}}{r} - (D-2) \frac{Q\sqrt{f}}{2r^{D-2}} \right) \right) \Psi_{\theta_2} &= i\omega \Psi_{\theta_1}. \end{aligned} \quad (3.24)$$

Setting

$$\tilde{\Psi}_{\theta_1} = r^{\frac{D-4}{2}} f^{\frac{1}{4}} \Psi_{\theta_1} \quad \text{and} \quad \tilde{\Psi}_{\theta_2} = r^{\frac{D-4}{2}} f^{\frac{1}{4}} \Psi_{\theta_2}, \quad (3.25)$$

we can simplify the equations in Eq. (3.24), and get the following,

$$(f\partial_r - \mathbb{W}) \tilde{\Psi}_{\theta_1} = i\omega \tilde{\Psi}_{\theta_1}, \quad (f\partial_r + \mathbb{W}) \tilde{\Psi}_{\theta_2} = i\omega \tilde{\Psi}_{\theta_2}, \quad (3.26)$$

where

$$\mathbb{W} = \frac{\bar{\zeta}\sqrt{f}}{r} - (D-2) \frac{Q\sqrt{f}}{2r^{D-2}}. \quad (3.27)$$

We now decouple the equations in Eq. (3.26) and obtain the radial equations

$$\begin{aligned} -\frac{d}{dr_*} \tilde{\Psi}_{\theta_1} + \mathbb{V}_1 \tilde{\Psi}_{\theta_1} &= \omega^2 \tilde{\Psi}_{\theta_1} \quad \text{and} \\ -\frac{d^2}{dr_*^2} \tilde{\Psi}_{\theta_2} + \mathbb{V}_2 \tilde{\Psi}_{\theta_2} &= \omega^2 \tilde{\Psi}_{\theta_2}, \end{aligned} \quad (3.28)$$

where

$$\mathbb{V}_{1,2} = \pm f(r) \frac{d\mathbb{W}}{dr} + \mathbb{W}^2$$

and our eigenvalue $\bar{\zeta}$ is given as $\bar{\zeta} = j + (D-3)/2$ with $j = 3/2, 5/2, 7/2, \dots$

As noted in Ref. [4], the Schwarzschild case of this potential is the same as for Dirac particles in a general dimensional Schwarzschild black hole [10]. This, however, is not true for the Reissner-Nordström case. For the spin-3/2 field one needs to use the supercovariant derivative in the charged black hole spacetime, whereas for the Dirac field one would still use the ordinary covariant derivative. The extra terms in the supercovariant derivative would render the effective potential of the spin-3/2 field in the TT mode to be different from that of the Dirac field in the same spacetime.

IV. QNMS

In order to obtain the QNMs we have chosen to use the WKB method, to third and sixth order, and the AIM. We investigate how the quasinormal frequencies change with the charge Q of the black hole, where a particularly interesting case of the Reissner-Nordström black hole would be the extremal case $Q = M$. In this section we present the QNMs in the cases $Q = 0.1M$, $Q = 0.5M$, and $Q = M$ for both “non-TT eigenfunction related” and “TT eigenfunction related” potentials from $D = 4$ to $D = 7$.

A. Non-TT eigenfunctions related

In this subsection we consider the QNMs of the radial equations in Eq. (3.20). Since V_1 and V_2 are isospectral, we can choose either one to work with. Here we concentrate on the first equation, that is, the potential V_1 . In the case of the WKB methods for the QNMs associated to the non-TT eigenfunctions, for the full explanation of how to determine the QNMs see Refs. [6,11]. For the AIM, a detailed discussion can be found in Refs. [3,4,7].

For the case of the Reissner-Nordström background, we start with the definition of the tortoise coordinate

$$\begin{aligned} dr_* &= \frac{1}{f(r)} dr, \\ f(r) &= 1 - \frac{2M}{r^{(D-3)}} + \frac{Q^2}{r^{2(D-3)}} \\ &= \frac{(r^{(D-3)} - r_+^{(D-3)})(r^{(D-3)} - r_-^{(D-3)})}{r^{2(D-3)}}, \end{aligned} \quad (4.1)$$

where $r_{\pm}^{(D-3)} = M \pm \sqrt{M^2 - Q^2}$. Taking $M = 1$, the relation between r and r_* is given by

$$\begin{aligned} r_* &= \int dr + \int \frac{2r_+^{(D-3)} - (r_+ r_-)^{(D-3)}}{(r_+^{(D-3)} - r_-^{(D-3)})(r^{(D-3)} - r_+^{(D-3)})} dr \\ &\quad + \int \frac{-2r_-^{(D-3)} + (r_+ r_-)^{(D-3)}}{(r_+^{(D-3)} - r_-^{(D-3)})(r^{(D-3)} - r_-^{(D-3)})} dr, \quad \text{for } Q < 1, \end{aligned} \quad (4.2)$$

$$r_* = \int \frac{r^{2(D-3)}}{r^{2(D-3)} - 2r^{(D-3)} + 1} dr, \quad \text{for } Q = 1. \quad (4.3)$$

In the AIM we first single out the asymptotic behavior of $\tilde{\phi}_1$, which is due to the QNM boundary conditions,

$$\tilde{\phi}_1 \rightarrow e^{\pm i\omega r_*} \sim \alpha, \quad r \rightarrow \pm\infty. \quad (4.4)$$

Note that we use “ \sim ” to signify that for convenience we choose the asymptotic function α to include the leading term and some of the subleading terms of $e^{\pm i\omega r_*}$, but

not necessarily the whole exponential. Next, a necessary coordinate transformation in the AIM is

$$\xi^2(r) = 1 - \frac{r_+}{r}. \quad (4.5)$$

The coefficients for the lowest order can be obtained as

$$\begin{aligned} \lambda_0 &= -\left(\frac{f'}{f} + \frac{\xi''}{\xi} + \frac{2\alpha'}{\alpha}\right), \\ s_0 &= -\left[\frac{\omega^2 - V}{f'\xi^2} + \frac{\alpha''}{\alpha} + \left(\frac{f'}{f} + \frac{\xi''}{\xi}\right)\frac{\alpha'}{\alpha}\right]. \end{aligned} \quad (4.6)$$

We next find the higher order λ and s by the relation

$$\lambda_n = \lambda'_{n-1} + s_{n-1} + \lambda_0 \lambda_{n-1}; \quad s_n = s'_{n-1} + s_0 \lambda_{n-1}, \quad (4.7)$$

and the corresponding ω by the equation

$$s_n \lambda_{n+1} - s_{n+1} \lambda_n = 0. \quad (4.8)$$

Note that

$$\begin{aligned} f' &= \frac{d}{d\xi} f(\xi), \quad \xi' = \frac{d}{dr} \xi(r) \Big|_{r=\frac{r_+}{1-\xi^2}}, \\ \xi'' &= \frac{d}{d\xi} \xi', \quad \alpha' = \frac{d}{d\xi} \alpha(\xi). \end{aligned} \quad (4.9)$$

Iterating this method for a sufficiently large number of iteration, ω becomes stable, indicating that this is the QNM we are looking for. For example, for the first mode of the extremal case in six dimensions, the relation between iteration number and the QNM frequency is plotted in Fig. 1 (with $M = 1$). This mode is one of the modes that the third and the sixth order WKB methods do not give a reasonable result for, but the AIM does.

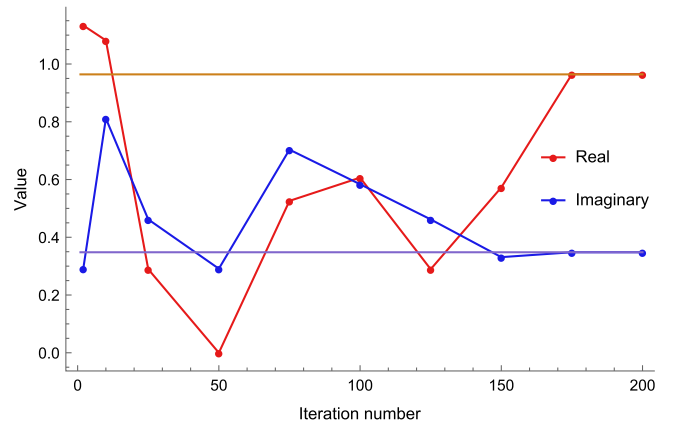


FIG. 1. The relation between iteration number and the value of the real part and the imaginary part of the QNM frequency for $j = 3/2$, $Q = 1$, and $D = 6$.

In Tables I–VI we present the QNMs for the Reissner-Nordström black hole for dimensions $D = 4$ to $D = 7$. The results are given in units of M , that is, we have set $M = 1$. We note that as the value of n increases, for fixed values of l ($= j - 3/2$) and D , the real part of the QNM decreases and the magnitude of the imaginary part increases, this being the same behavior as we have seen for the Schwarzschild black hole. This result suggests that the lower modes are easier to detect compared to the higher less energetic modes. Furthermore, they also decay the slowest. We also note that an increase in the number of dimensions results in the QNM being emitted more energetically. This can be understood by considering the change in the potentials as the dimension is increased as shown in Fig. 2. From $D = 4$ to $D = 7$ the maximum value of the potential increases as D is increased. Hence, the real part of the QNM frequency would also increase. Lastly, when the charge Q is increased, the real part of the frequency for the same mode increases, while the magnitude of the imaginary part also increases. This is consistent with the change of the effective potentials as Q is increased, as shown in Fig. 3. As Q is increased from 0 to 1 (in units of M), the maximum value of the potential increases; hence the real part of the QNM frequency increases. On the other hand, the potential tends to sharpen as Q is increased; this implies that the field can decay more easily, giving a large decay constant, or a large absolute value of the imaginary part of the frequency.

Note that in the tables there are several blank entries. The reason for leaving these entries out is that we think the numbers we have obtained are not reliable. For the WKB approximation we found that higher order terms dominate over the lower order terms. This is unreasonable as the WKB method is generated from a series expansion. As for the AIM, the results do not converge when the number of iterations is increased. As such, in these cases we have left these entries as blank.

We also find that there is a strong disagreement for the WKB methods in the cases of $Q = M$, for dimensions higher than 7. The reason for this disagreement is twofold. The first is again the problem with the WKB series expansion, as mentioned above. The second one is due to the peculiar behavior of the effective potential. As shown in Fig. 2, it is clear that for the $j = 3/2$ potentials in the cases $D > 7$, a second local maximum will develop. This happens not just for the $j = 3/2$ cases but also for potentials with other j values. For larger values of j , the dimension at which the potential will have this behavior is higher. The presence of a second maximum renders the WKB approximation and the AIM unreliable, so we have only listed the results up to $D = 7$ in these instances.

B. TT eigenfunctions related

For the TT eigenfunction related cases, both the WKB and AIM present reasonable results. We have to note that

TABLE I. Low-lying ($n \leq l$, with $l = j - 3/2$) spin-3/2 field quasinormal frequencies using the WKB and the AIM with $D = 4, 5$ and $Q = 0.1 M$.

Four dimensions					Five dimensions				
l	n	WKB third order	WKB sixth order	AIM	l	n	WKB third order	WKB sixth order	AIM
0	0	0.3161-0.0909i	0.3185-0.0910i	0.3185-0.0909i	0	0	0.6360-0.2147i	0.6484-0.2191i	0.6484-0.2191i
1	0	0.5370-0.0942i	0.5375-0.0942i	0.5374-0.0942i	1	0	1.0773-0.2343i	1.0808-0.2343i	1.0807-0.2343i
1	1	0.5180-0.2871i	0.5191-0.2867i	0.5191-0.2867i	1	1	0.9917-0.7241i	1.0008-0.7209i	1.0008-0.7209i
2	0	0.7423-0.0952i	0.7425-0.0952i	0.7424-0.0952i	2	0	1.4730-0.2411i	1.4742-0.2411i	1.4742-0.2411i
2	1	0.7285-0.2880i	0.7289-0.2879i	0.7289-0.2878i	2	1	1.4100-0.7347i	1.4126-0.7342i	1.4126-0.7342i
2	2	0.7041-0.4860i	0.7035-0.4871i	0.7034-0.4870i	2	2	1.2998-1.2522i	1.2922-1.2636i	1.2922-1.2636i
3	0	0.9423-0.0957i	0.9424-0.0957i	0.9424-0.0956i	3	0	1.8520-0.2443i	1.8527-0.2443i	1.8527-0.2443i
3	1	0.9315-0.2884i	0.9316-0.2884i	0.9316-0.2883i	3	1	1.8018-0.7401i	1.8040-0.7395i	1.8040-0.7395i
3	2	0.9114-0.4848i	0.9109-0.4853i	0.9109-0.4852i	3	2	1.7104-1.2530i	1.7101-1.2546i	1.7101-1.2546i
3	3	0.8845-0.6853i	0.8819-0.6887i	0.8819-0.6887i	3	3	1.5882-1.7838i	1.5787-1.8012i	1.5787-1.8012i
4	0	1.1398-0.0959i	1.1399-0.0959i	1.1398-0.0958i	4	0	2.2228-0.2461i	2.2232-0.2461i	2.2232-0.2461i
4	1	1.1309-0.2886i	1.1310-0.2886i	1.1309-0.2886i	4	1	2.1809-0.7432i	2.1824-0.7429i	2.1824-0.7429i
4	2	1.1139-0.4840i	1.1136-0.4842i	1.1135-0.4842i	4	2	2.1027-1.2530i	2.1031-1.2534i	2.1031-1.2534i
4	3	1.0905-0.6827i	1.0886-0.6845i	1.0886-0.6845i	4	3	1.9958-1.7778i	1.9911-1.7852i	1.9911-1.7852i
4	4	1.0620-0.8848i	1.0575-0.8910i	1.0575-0.8909i	4	4	1.8659-2.3161i	1.8545-2.3415i	1.8545-2.3415i
5	0	1.3360-0.0960i	1.3360-0.0960i	1.3360-0.0960i	5	0	2.5889-0.2471i	2.5891-0.2471i	2.5891-0.2471i
5	1	1.3283-0.2887i	1.3284-0.2887i	1.3283-0.2887i	5	1	2.5529-0.7451i	2.5536-0.7450i	2.5536-0.7450i
5	2	1.3136-0.4834i	1.3134-0.4836i	1.3133-0.4835i	5	2	2.4846-1.2528i	2.4838-1.2536i	2.4838-1.2536i
5	3	1.2929-0.6809i	1.2916-0.6819i	1.2916-0.6819i	5	3	2.3895-1.7731i	2.3822-1.7802i	2.3822-1.7802i
5	4	1.2674-0.8812i	1.2640-0.8849i	1.2640-0.8849i	5	4	2.2727-2.3056i	2.2533-2.3315i	2.2533-2.3315i
5	5	1.2378-1.0842i	1.2315-1.0935i	1.2315-1.0935i	5	5	2.1371-2.8485i	2.1024-2.9129i	2.1024-2.9129i

TABLE II. Low-lying ($n \leq l$, with $l = j - 3/2$) spin-3/2 field quasinormal frequencies using the WKB and the AIM with $D = 6$, 7 and $Q = 0.1$ M

Six dimensions					Seven dimensions				
l	n	WKB third order	WKB sixth order	AIM	l	n	WKB third order	WKB sixth order	AIM
0	0	0.9364-0.3422i	0.9408-0.3027i	0.9408-0.3027i	0	0	1.2845-0.4857i	1.2111-0.5136i	1.2110-0.5136i
1	0	1.5164-0.3578i	1.5292-0.3540i	1.5292-0.3540i	1	0	1.9288-0.4776i	1.9388-0.4621i	1.9388-0.4621i
1	1	1.3214-1.1165i	1.3680-1.0786i	1.3680-1.0786i	1	1	1.5920-1.4970i	1.6160-1.3961i	1.6160-1.3961i
2	0	2.0379-0.3705i	2.0418-0.3699i	2.0418-0.3699i	2	0	2.5348-0.4880i	2.5430-0.4836i	2.5430-0.4836i
2	1	1.8967-1.1346i	1.9117-1.1279i	1.9117-1.1279i	2	1	2.2870-1.4974i	2.3243-1.4620i	2.3243-1.4620i
2	2	1.6451-1.9511i	1.6488-1.9502i	1.6488-1.9502i	2	2	1.8288-2.5991i	1.8401-2.5026i	1.8401-2.5026i
3	0	2.5341-0.3774i	2.5360-0.3772i	2.5360-0.3772i	3	0	3.1136-0.4968i	3.1174-0.4954i	3.1174-0.4954i
3	1	2.4214-1.1470i	2.4285-1.1444i	2.4285-1.1444i	3	1	2.9167-1.5115i	2.9352-1.5003i	2.9352-1.5003i
3	2	2.2133-1.9532i	2.2124-1.9547i	2.2124-1.9547i	3	2	2.5422-2.5869i	2.5506-2.5600i	2.5506-2.5600i
3	3	1.9314-2.8004i	1.8910-2.8487i	1.8910-2.8487i	3	3	2.0267-3.7434i	1.9395-3.7554i	1.9395-3.7554i
4	0	3.0173-0.3816i	3.0183-0.3814i	3.0183-0.3814i	4	0	3.6764-0.5028i	3.6784-0.5022i	3.6784-0.5022i
4	1	2.9227-1.1550i	2.9267-1.1537i	2.9267-1.1537i	4	1	3.5114-1.5233i	3.5215-1.5186i	3.5215-1.5186i
4	2	2.7444-1.9555i	2.7428-1.9567i	2.7428-1.9567i	4	2	3.1931-2.5872i	3.1959-2.5773i	3.1959-2.5773i
4	3	2.4979-2.7896i	2.4678-2.8176i	2.4678-2.8176i	4	3	2.7445-3.7136i	2.6843-3.7312i	2.6843-3.7312i
4	4	2.1951-3.6553i	2.1087-3.7702i	2.1087-3.7702i	4	4	2.1908-4.9064i	1.9854-5.0614i	1.9854-5.0614i
5	0	3.4926-0.3842i	3.4932-0.3841i	3.4932-0.3841i	5	0	4.2293-0.5070i	4.2305-0.5067i	4.2305-0.5067i
5	1	3.4109-1.1603i	3.4133-1.1596i	3.4133-1.1596i	5	1	4.0865-1.5321i	4.0927-1.5296i	4.0927-1.5296i
5	2	3.2547-1.9572i	3.2531-1.9581i	3.2531-1.9581i	5	2	3.8085-2.5899i	3.8092-2.5851i	3.8092-2.5851i
5	3	3.0353-2.7818i	3.0130-2.7991i	3.0130-2.7991i	5	3	3.4108-3.6971i	3.3672-3.7097i	3.3672-3.7097i
5	4	2.7630-3.6346i	2.6964-3.7065i	2.6964-3.7065i	5	4	2.9125-4.8608i	2.7597-4.9595i	2.7597-4.9595i
5	5	2.4444-4.5127i	2.3116-4.7073i	2.3116-4.7073i	5	5	2.3296-6.0794i	1.9987-6.4037i	1.9987-6.4037i

TABLE III. Low-lying ($n \leq l$, with $l = j - 3/2$) spin-3/2 field quasinormal frequencies using the WKB and the AIM with $D = 4$, 5 and $Q = 0.5$ M.

Four dimensions					Five dimensions				
l	n	WKB third order	WKB sixth order	AIM	l	n	WKB third order	WKB sixth order	AIM
0	0	0.3616-0.0953i	0.3634-0.0952i	0.3621-0.0881i	0	0	0.7048-0.2213i	0.8005-0.1499i	0.7065-0.2259i
1	0	0.5905-0.0971i	0.5908-0.0971i	0.4050-0.1854i	1	0	1.1471-0.2356i	1.1504-0.2347i	1.1504-0.2346i
1	1	0.5736-0.2950i	0.5744-0.2948i	0.3674-0.3656i	1	1	1.0756-0.7253i	1.0842-0.7160i	1.0842-0.7159i
2	0	0.8044-0.0976i	0.8046-0.0976i	0.8045-0.0975i	2	0	1.5506-0.2420i	1.5519-0.2420i	1.5519-0.2420i
2	1	0.7920-0.2948i	0.7923-0.2947i	0.7922-0.2947i	2	1	1.4946-0.7364i	1.4995-0.7345i	1.4995-0.7345i
2	2	0.7698-0.4967i	0.7692-0.4977i	0.7691-0.4976i	2	2	1.3974-1.2527i	1.4031-1.2505i	1.4031-1.2505i
3	0	1.0131-0.0977i	1.0132-0.0977i	1.0131-0.0977i	3	0	1.9368-0.2448i	1.9374-0.2448i	1.9374-0.2448i
3	1	1.0032-0.2945i	1.0033-0.2945i	1.0033-0.2944i	3	1	1.8913-0.7411i	1.8931-0.7408i	1.8931-0.7408i
3	2	0.9849-0.4946i	0.9844-0.4950i	0.9844-0.4950i	3	2	1.8088-1.2532i	1.8074-1.2559i	1.8074-1.2559i
3	3	0.9602-0.6986i	0.9579-0.7015i	0.9579-0.7015i	3	3	1.6992-1.7820i	1.6869-1.8027i	1.6869-1.8027i
4	0	1.2193-0.0978i	1.2193-0.0978i	1.2193-0.0978i	4	0	2.3142-0.2462i	2.3145-0.2462i	2.3145-0.2462i
4	1	1.2110-0.2943i	1.2111-0.2943i	1.2111-0.2942i	4	1	2.2759-0.7433i	2.2770-0.7432i	2.2770-0.7432i
4	2	1.1954-0.4932i	1.1951-0.4934i	1.1951-0.4934i	4	2	2.2047-1.2523i	2.2036-1.2538i	2.2036-1.2538i
4	3	1.1738-0.6952i	1.1722-0.6968i	1.1722-0.6967i	4	3	2.1077-1.7753i	2.0983-1.7871i	2.0983-1.7871i
4	4	1.1476-0.9004i	1.1437-0.9057i	1.1437-0.9057i	4	4	1.9902-2.3108i	1.9669-2.3518i	1.9669-2.3518i
5	0	1.4240-0.0978i	1.4241-0.0978i	1.4241-0.0978i	5	0	2.6865-0.2470i	2.6868-0.2470i	2.6868-0.2470i
5	1	1.4170-0.2941i	1.4170-0.2941i	1.4170-0.2941i	5	1	2.6535-0.7445i	2.6542-0.7444i	2.6542-0.7444i
5	2	1.4034-0.4922i	1.4032-0.4923i	1.4032-0.4923i	5	2	2.5910-1.2510i	2.5901-1.2519i	2.5901-1.2519i
5	3	1.3843-0.6928i	1.3831-0.6937i	1.3831-0.6937i	5	3	2.5041-1.7694i	2.4970-1.7766i	2.4970-1.7766i
5	4	1.3606-0.8962i	1.3576-0.8994i	1.3576-0.8994i	5	4	2.3977-2.2993i	2.3787-2.3250i	2.3787-2.3250i
5	5	1.3333-1.1022i	1.3277-1.1101i	1.3277-1.1101i	5	5	2.2747-2.8389i	2.2403-2.9032i	2.2403-2.9032i

TABLE IV. Low-lying ($n \leq l$, with $l = j - 3/2$) spin-3/2 field quasinormal frequencies using the WKB and the AIM with $D = 6$, 7 and $Q = 0.5$ M.

Six dimensions					Seven dimensions				
l	n	WKB third order	WKB sixth order	AIM	l	n	WKB third order	WKB sixth order	AIM
0	0	0.9546-0.1667i		0.9545-0.1666i	0	0	1.1968-0.3978i		1.1967-0.3978i
1	0	1.5887-0.3502i	1.5411-0.3743i	1.5411-0.3743i	1	0	1.9675-0.4197i		
1	1	1.4709-1.0935i	1.2200-1.3800i	1.2200-1.3800i	1	1	1.6232-1.2937i		
2	0	2.1178-0.3667i	2.1190-0.3673i	2.1190-0.3673i	2	0	2.6056-0.4703i	2.5998-0.4897i	2.5998-0.4897i
2	1	2.0024-1.1232i	2.0024-1.1224i	2.0024-1.1224i	2	1	2.4023-1.4443i	2.3449-1.6313i	2.3449-1.6313i
2	2	1.8050-1.9277i	1.7720-1.9392i	1.7720-1.9392i	2	2	2.0392-2.4977i	1.9354-3.3791i	1.9354-3.3791i
3	0	2.6220-0.3750i	2.6235-0.3751i	2.6235-0.3751i	3	0	3.1972-0.4877i	3.1984-0.4909i	3.1984-0.4909i
3	1	2.5225-1.1395i	2.5271-1.1384i	2.5271-1.1384i	3	1	3.0274-1.4858i	3.0248-1.5096i	3.0248-1.5096i
3	2	2.3417-1.9388i	2.3351-1.9436i	2.3351-1.9436i	3	2	2.7137-2.5414i	2.6649-2.6679i	2.6649-2.6679i
3	3	2.1010-2.7748i	2.0523-2.8252i	2.0523-2.8252i	3	3	2.2912-3.6638i	2.1445-4.1160i	2.1445-4.1160i
4	0	3.1119-0.3795i	3.1129-0.3796i	3.1129-0.3796i	4	0	3.7688-0.4968i	3.7706-0.4975i	3.7706-0.4975i
4	1	3.0261-1.1488i	3.0295-1.1482i	3.0295-1.1482i	4	1	3.6211-1.5062i	3.6269-1.5094i	3.6269-1.5094i
4	2	2.8655-1.9440i	2.8632-1.9468i	2.8632-1.9468i	4	2	3.3407-2.5582i	3.3302-2.5804i	3.3302-2.5804i
4	3	2.6457-2.7704i	2.6165-2.8004i	2.6165-2.8004i	4	3	2.9521-3.6661i	2.8719-3.7744i	2.8719-3.7744i
4	4	2.3779-3.6250i	2.2969-3.7378i	2.2969-3.7378i	4	4	2.4763-4.8284i	2.2632-5.1748i	2.2632-5.1748i
5	0	3.5931-0.3823i	3.5937-0.3823i	3.5937-0.3823i	5	0	4.3286-0.5023i	4.3299-0.5025i	4.3299-0.5025i
5	1	3.5180-1.1543i	3.5204-1.1540i	3.5204-1.1540i	5	1	4.1979-1.5186i	4.2034-1.5187i	4.2034-1.5187i
5	2	3.3751-1.9464i	3.3738-1.9481i	3.3738-1.9481i	5	2	3.9462-2.5673i	3.9440-2.5725i	3.9440-2.5725i
5	3	3.1756-2.7646i	3.1555-2.7829i	3.1555-2.7829i	5	3	3.5902-3.6620i	3.5428-3.7021i	3.5428-3.7021i
5	4	2.9296-3.6087i	2.8698-3.6796i	2.8698-3.6796i	5	4	3.1475-4.8060i	2.9968-4.9618i	2.9968-4.9618i
5	5	2.6429-4.4752i	2.5247-4.6616i	2.5247-4.6616i	5	5	2.6308-5.9957i	2.3192-6.4154i	2.3192-6.4154i

TABLE V. Low-lying ($n \leq l$, with $l = j - 3/2$) spin-3/2 field quasinormal frequencies using the WKB and the AIM with $D = 4$, 5 and $Q = M$.

Four dimensions					Five dimensions				
l	n	WKB third order	WKB sixth order	AIM	l	n	WKB third order	WKB sixth order	AIM
0	0	0.5410-0.0867i	0.5414-0.0865i	0.5414-0.0864i	0	0	0.8519-0.1875i		
1	0	0.8173-0.0874i	0.8174-0.0874i	0.8174-0.0873i	1	0	1.3394-0.2077i	1.3414-0.2098i	1.3413-0.2097i
1	1	0.8027-0.2638i	0.8032-0.2636i	0.8032-0.2636i	1	1	1.2704-0.6320i	1.2809-0.6422i	1.2809-0.6422i
2	0	1.0810-0.0878i	1.0811-0.0878i	1.0811-0.0877i	2	0	1.7723-0.2144i	1.7735-0.2147i	1.7735-0.2147i
2	1	1.0701-0.2643i	1.0704-0.2643i	1.0703-0.2642i	2	1	1.7224-0.6490i	1.7266-0.6494i	1.7266-0.6494i
2	2	1.0491-0.4435i	1.0491-0.4435i	1.0490-0.4435i	2	2	1.6288-1.0985i	1.6337-1.1014i	1.6337-1.1014i
3	0	1.3395-0.0880i	1.3396-0.0880i	1.3395-0.0879i	3	0	2.1865-0.2174i	2.1872-0.2175i	2.1872-0.2175i
3	1	1.3307-0.2646i	1.3309-0.2646i	1.3308-0.2645i	3	1	2.1461-0.6559i	2.1486-0.6558i	2.1486-0.6558i
3	2	1.3136-0.4430i	1.3136-0.4430i	1.3135-0.4430i	3	2	2.0689-1.1048i	2.0716-1.1049i	2.0716-1.1049i
3	3	1.2889-0.6239i	1.2880-0.6245i	1.2880-0.6245i	3	3	1.9604-1.5675i	1.9574-1.5732i	1.9574-1.5732i
4	0	1.5953-0.0881i	1.5953-0.0881i	1.5953-0.0881i	4	0	2.5913-0.2189i	2.5917-0.2190i	2.5917-0.2190i
4	1	1.5879-0.2648i	1.5880-0.2648i	1.5880-0.2648i	4	1	2.5572-0.6595i	2.5587-0.6594i	2.5587-0.6594i
4	2	1.5734-0.4427i	1.5734-0.4427i	1.5734-0.4427i	4	2	2.4912-1.1076i	2.4929-1.1075i	2.4929-1.1075i
4	3	1.5523-0.6225i	1.5517-0.6228i	1.5517-0.6228i	4	3	2.3969-1.5663i	2.3948-1.5691i	2.3948-1.5691i
4	4	1.5252-0.8047i	1.5232-0.8060i	1.5232-0.8060i	4	4	2.2784-2.0370i	2.2655-2.0507i	2.2655-2.0507i
5	0	1.8494-0.0882i	1.8494-0.0882i	1.8494-0.0882i	5	0	2.9905-0.2199i	2.9908-0.2199i	2.9908-0.2199i
5	1	1.8430-0.2649i	1.8431-0.2649i	1.8431-0.2649i	5	1	2.9610-0.6616i	2.9620-0.6616i	2.9620-0.6616i
5	2	1.8305-0.4425i	1.8305-0.4425i	1.8305-0.4425i	5	2	2.9034-1.1090i	2.9045-1.1090i	2.9045-1.1090i
5	3	1.8121-0.6216i	1.8117-0.6218i	1.8117-0.6218i	5	3	2.8201-1.5649i	2.8186-1.5665i	2.8186-1.5665i
5	4	1.7883-0.8026i	1.7869-0.8034i	1.7869-0.8034i	5	4	2.7143-2.0307i	2.7049-2.0388i	2.7049-2.0388i
5	5	1.7596-0.9857i	1.7563-0.9879i	1.7563-0.9879i	5	5	2.5887-2.5066i	2.5646-2.5311i	2.5646-2.5311i

TABLE VI. Low-lying ($n \leq l$, with $l = j - 3/2$) spin-3/2 field quasinormal frequencies using the WKB and the AIM with $D = 6, 7$ and $Q = M$.

Six dimensions					Seven dimensions				
l	n	WKB third order	WKB sixth order	AIM	l	n	WKB third order	WKB sixth order	AIM
0	0			0.9646–0.3481i	0	0			
1	0	1.7521–0.3082i		1.7516–0.3053i	1	0			
1	1	1.6678–0.9419i		1.6970–0.9918i	1	1			
2	0	2.3058–0.3275i	2.3115–0.3240i	2.3081–0.3401i	2	0	2.7749–0.4333i	2.8918–0.3419i	2.7749–0.4333i
2	1	2.2126–0.9992i	2.2297–0.9708i	2.2375–1.0523i	2	1	2.7194–1.3659i		2.7194–1.3659i
2	2	2.0483–1.7097i	2.0302–1.6426i	2.1478–1.8272i	2	2	2.7162–2.4111i		2.7162–2.4111i
3	0	2.8322–0.3371i	2.8345–0.3368i	2.8345–0.3368i	3	0	3.3789–0.4424i	3.3883–0.4341i	3.3883–0.4341i
3	1	2.7461–1.0212i	2.7554–1.0156i	2.7554–1.0156i	3	1	3.2568–1.3524i	3.3296–1.2462i	3.3296–1.2462i
3	2	2.5841–1.7318i	2.5948–1.7106i	2.5948–1.7106i	3	2	3.0467–2.3221i		3.3425–1.7230i
3	3	2.3621–2.4758i	2.3449–2.4367i	2.3449–2.4367i	3	3	2.7896–3.3500i		3.9401–1.1831i
4	0	3.3424–0.3426i	3.3438–0.3426i	3.3438–0.3426i	4	0	3.9683–0.4525i	3.9713–0.4516i	3.9713–0.4516i
4	1	3.2663–1.0344i	3.2720–1.0332i	3.2720–1.0332i	4	1	3.8448–1.3713i	3.8600–1.3555i	3.8600–1.3555i
4	2	3.1198–1.7450i	3.1269–1.7402i	3.1269–1.7402i	4	2	3.6112–2.3277i	3.6410–2.2421i	3.6410–2.2421i
4	3	2.9124–2.4820i	2.9058–2.4774i	2.9058–2.4774i	4	3	3.2891–3.3340i	3.3018–3.0389i	3.3018–3.0389i
4	4	2.6545–3.2475i	2.6054–3.2637i	2.6054–3.2637i	4	4	2.8991–4.3888i	2.7814–3.5851i	2.7814–3.5851i
5	0	3.8425–0.3459i	3.8435–0.3460i	3.8435–0.3460i	5	0	4.5446–0.4595i	4.5466–0.4595i	4.5466–0.4595i
5	1	3.7753–1.0426i	3.7792–1.0422i	3.7792–1.0422i	5	1	4.4302–1.3874i	4.4389–1.3841i	4.4389–1.3841i
5	2	3.6441–1.7533i	3.6494–1.7517i	3.6494–1.7517i	5	2	4.2074–2.3414i	4.2195–2.3230i	4.2195–2.3230i
5	3	3.4554–2.4847i	3.4524–2.4854i	3.4524–2.4854i	5	3	3.8883–3.3348i	3.8773–3.2798i	3.8773–3.2798i
5	4	3.2166–3.2404i	3.1862–3.2573i	3.1862–3.2573i	5	4	3.4880–4.3739i	3.3887–4.2548i	3.3887–4.2548i
5	5	2.9346–4.0206i	2.8505–4.0854i	2.8505–4.0854i	5	5	3.0202–5.4581i	2.7165–5.2505i	2.7165–5.2505i

there is no TT eigenfunction related case in the four-dimensional Reissner-Nordström spacetime because of the absence of the TT eigenmodes on the 2-sphere. In Tables VII–XII we present the TT QNMs for $Q = 0.1M$, $Q = 0.5M$, and $Q = M$ from $D = 5$ to $D = 7$. The change in QNM frequencies is similar to that for non-TT cases when either n or D is changed. To see how the frequencies are affected by the change in the charge Q , we plot in Fig. 4 the first three modes in more detail for $Q = 0$ to 1. The red, blue and green colors represent five, six, and seven dimensions. The result indicates that when Q becomes

larger, the real part decreases and the absolute value of the imaginary part also decreases. This is consistent with the change of the TT potential with Q , which is plotted in Fig. 5. We can see that when Q is increased, the maximum value of the potential decreases. This implies that the real part of the QNM frequency decreases accordingly. In addition to this the potential broadens when Q is increased, so the mode decays slower, which implies that the absolute value of the imaginary part of the frequency becomes smaller. Note that this trend is the exact opposite to that for the non-TT cases for $D < 7$.

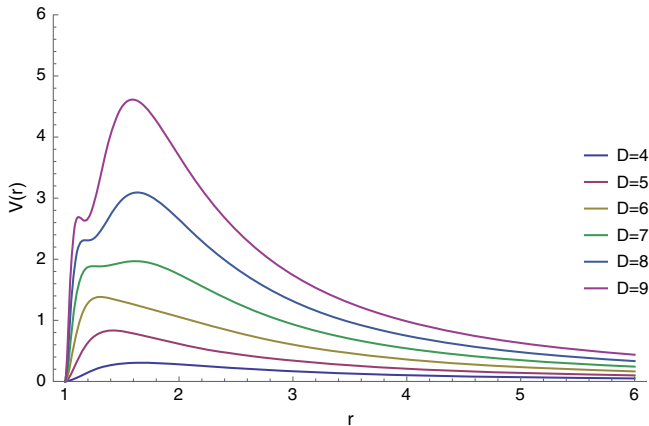
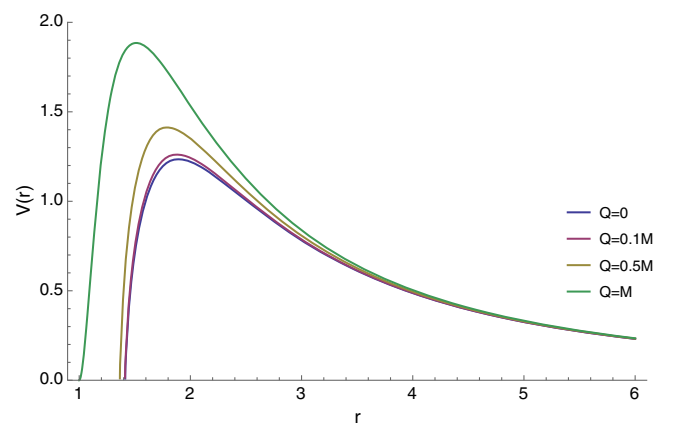
FIG. 2. Potential function with $j = 3/2$ and $Q = 1$ for $D = 4$ to $D = 9$.FIG. 3. The non-TT effective potential with $D = 5$ and $j = 5/2$ for $Q = 0$ to $Q = 1$.

TABLE VII. Low-lying ($n \leq l$, with $l = j - 3/2$) spin-3/2 field quasinormal frequencies using the WKB and the AIM with $D = 5$ and $Q = 0.1$ M.

Five dimensions				
l	n	WKB third order	WKB sixth order	AIM
0	0	0.8443-0.2482i	0.8538-0.2493i	0.7755-0.1916i
1	0	1.2093-0.2487i	1.2124-0.2490i	1.2355-0.2633i
1	1	1.1297-0.7659i	1.1384-0.7640i	0.8044-0.6729i
2	0	1.5677-0.2490i	1.5690-0.2490i	1.5690-0.2490i
2	1	1.5069-0.7580i	1.5108-0.7572i	1.5108-0.7572i
2	2	1.4010-1.2904i	1.4002-1.2962i	1.4002-1.2962i
3	0	1.9239-0.2492i	1.9245-0.2492i	1.9245-0.2492i
3	1	1.8747-0.7545i	1.8767-0.7541i	1.8767-0.7541i
3	2	1.7854-1.2767i	1.7840-1.2795i	1.7840-1.2795i
3	3	1.6663-1.8167i	1.6530-1.8392i	1.6530-1.8392i
4	0	2.2791-0.2493i	2.2795-0.2493i	2.2795-0.2493i
4	1	2.2379-0.7527i	2.2390-0.7525i	2.2390-0.7525i
4	2	2.1608-1.2687i	2.1596-1.2703i	2.1596-1.2703i
4	3	2.0557-1.7997i	2.0451-1.8126i	2.0451-1.8126i
4	4	1.9280-2.3440i	1.9017-2.3890i	1.9017-2.3890i
5	0	2.6340-0.2493i	2.6342-0.2493i	2.6342-0.2493i
5	1	2.5983-0.7517i	2.5990-0.7516i	2.5990-0.7516i
5	2	2.5307-1.2637i	2.5297-1.2647i	2.5297-1.2647i
5	3	2.4367-1.7883i	2.4286-1.7961i	2.4286-1.7961i
5	4	2.3212-2.3250i	2.2998-2.3533i	2.2998-2.3533i
5	5	2.1873-2.8720i	2.1482-2.9430i	2.1482-2.9430i

TABLE VIII. Low-lying ($n \leq l$, with $l = j - 3/2$) spin-3/2 field quasinormal frequencies using the WKB and the AIM with $D = 6, 7$ and $Q = 0.1$ M.

Six dimensions					Seven dimensions				
l	n	WKB third order	WKB sixth order	AIM	l	n	WKB third order	WKB sixth order	AIM
0	0	1.2853-0.3861i	1.3064-0.3961i	1.3063-0.3961i	0	0	1.7137-0.5075i	1.7430-0.5408i	1.7430-0.5408i
1	0	1.7613-0.3889i	1.7692-0.3917i	1.7692-0.3917i	1	0	2.2717-0.5149i	2.2844-0.5247i	2.2844-0.5247i
1	1	1.5809-1.2099i	1.6097-1.2106i	1.6097-1.2106i	1	1	1.9511-1.6139i	2.0126-1.6368i	2.0126-1.6368i
2	0	2.2243-0.3901i	2.2281-0.3906i	2.2282-0.3904i	2	0	2.8099-0.5180i	2.8176-0.5196i	2.8176-0.5196i
2	1	2.0867-1.1939i	2.1008-1.1922i	2.1008-1.1922i	2	1	2.5668-1.5899i	2.6000-1.5911i	2.6000-1.5911i
2	2	1.8433-2.0498i	1.8483-2.0618i	1.8483-2.0618i	2	2	2.1240-2.7539i	2.1468-2.7766i	2.1468-2.7766i
3	0	2.6826-0.3906i	2.6846-0.3906i	2.6846-0.3906i	3	0	3.3403-0.5191i	3.3445-0.5191i	3.3445-0.5191i
3	1	2.5712-1.1868i	2.5787-1.1853i	2.5787-1.1853i	3	1	3.1444-1.5797i	3.1633-1.5766i	3.1633-1.5766i
3	2	2.3663-2.0196i	2.3672-2.0240i	2.3672-2.0240i	3	2	2.7746-2.7018i	2.7858-2.7031i	2.7858-2.7031i
3	3	2.0899-2.8930i	2.0549-2.9462i	2.0549-2.9462i	3	3	2.2680-3.9031i	2.1975-3.9815i	2.1975-3.9815i
4	0	3.1389-0.3909i	3.1400-0.3908i	3.1400-0.3908i	4	0	3.8673-0.5196i	3.8696-0.5194i	3.8696-0.5194i
4	1	3.0451-1.1830i	3.0493-1.1821i	3.0493-1.1821i	4	1	3.7024-1.5743i	3.7135-1.5716i	3.7135-1.5716i
4	2	2.8685-2.0023i	2.8678-2.0044i	2.8678-2.0044i	4	2	3.3855-2.6730i	3.3908-2.6705i	3.3908-2.6705i
4	3	2.6248-2.8550i	2.5975-2.8847i	2.5975-2.8847i	4	3	2.9404-3.8338i	2.8874-3.8700i	2.8874-3.8700i
4	4	2.3261-3.7390i	2.2457-3.8554i	2.2457-3.8554i	4	4	2.3917-5.0594i	2.2039-5.2494i	2.2039-5.2494i
5	0	3.5942-0.3910i	3.5948-0.3910i	3.5948-0.3910i	5	0	4.3926-0.5198i	4.3940-0.5197i	4.3940-0.5197i
5	1	3.5129-1.1808i	3.5156-1.1802i	3.5156-1.1802i	5	1	4.2497-1.5710i	4.2566-1.5691i	4.2566-1.5691i
5	2	3.3578-1.9914i	3.3567-1.9926i	3.3567-1.9926i	5	2	3.9722-2.6553i	3.9746-2.6529i	3.9746-2.6529i
5	3	3.1401-2.8297i	3.1191-2.8476i	3.1191-2.8476i	5	3	3.5760-3.7890i	3.5363-3.8079i	3.5363-3.8079i
5	4	2.8703-3.6960i	2.8067-3.7686i	2.8067-3.7686i	5	4	3.0802-4.9785i	2.9360-5.0898i	2.9360-5.0898i
5	5	2.5549-4.5872i	2.4278-4.7818i	2.4278-4.7818i	5	5	2.5001-6.2217i	2.1857-6.5663i	2.1857-6.5663i

C. Large angular momentum limit

In the previous sections we have seen that the fermionic QNMs in a Reissner-Nordström spacetime have a different set of solutions associated to either the spin-1/2 or the spin-3/2 particles, this being due to the fact that we have introduced a supercovariant derivative for the spin-3/2 case in order to satisfy the gauge symmetry. However, in our previous work we showed that the QNMs for the TT modes of the spin-3/2 particles coincide with those of the spin-1/2 particles [4]. In this section we expand on this analysis by considering the large angular limit of our potential.

To first order the large angular momentum limit for the QNMs can be approximated as

$$\omega \approx \left[V_0 - i \left(n + \frac{1}{2} \right) (-2V_0'')^{1/2} + \dots \right]^{1/2},$$

$$\sim V_0^{1/2} - i \left(n + \frac{1}{2} \right) \frac{(-2V_0'')^{1/2}}{2(V_0)^{1/2}} + \dots, \quad (4.10)$$

where V_0 is the maximum of the effective potential, and prime represents derivatives with respect to the tortoise coordinate r_* . The large angular momentum limit of the super potentials, Eqs. (3.19) and (3.27), and those in Refs. [4,10], have the same corresponding effective potential of the general form

TABLE IX. Low-lying ($n \leq l$, with $l = j - 3/2$) spin-3/2 field quasinormal frequencies using the WKB and the AIM with $D = 5$ and $Q = 0.5$ M.

Five dimensions				
l	n	WKB third order	WKB sixth order	AIM
0	0	0.8029-0.2388i	0.8131-0.2411i	0.3915-0.2511i
1	0	1.1737-0.2414i	1.1769-0.2418i	1.1768-0.2418i
1	1	1.0949-0.7434i	1.1046-0.7419i	1.1045-0.7419i
2	0	1.5374-0.2427i	1.5387-0.2428i	1.5387-0.2428i
2	1	1.4783-0.7388i	1.4825-0.7381i	1.4825-0.7381i
2	2	1.3751-1.2575i	1.3754-1.2628i	1.3754-1.2628i
3	0	1.8990-0.2436i	1.8996-0.2436i	1.8996-0.2436i
3	1	1.8516-0.7375i	1.8537-0.7372i	1.8537-0.7372i
3	2	1.7654-1.2475i	1.7647-1.2502i	1.7647-1.2502i
3	3	1.6504-1.7747i	1.6389-1.7957i	1.6389-1.7957i
4	0	2.2597-0.2442i	2.2601-0.2442i	2.2601-0.2442i
4	1	2.2202-0.7372i	2.2213-0.7370i	2.2213-0.7370i
4	2	2.1463-1.2422i	2.1454-1.2437i	2.1454-1.2437i
4	3	2.0453-1.7616i	2.0361-1.7736i	2.0361-1.7736i
4	4	1.9228-2.2938i	1.8992-2.3356i	1.8992-2.3356i
5	0	2.6201-0.2446i	2.6203-0.2446i	2.6203-0.2446i
5	1	2.5860-0.7373i	2.5867-0.7372i	2.5867-0.7372i
5	2	2.5214-1.2392i	2.5207-1.2400i	2.5207-1.2400i
5	3	2.4316-1.7530i	2.4245-1.7603i	2.4245-1.7603i
5	4	2.3212-2.2786i	2.3020-2.3048i	2.3020-2.3048i
5	5	2.1933-2.8141i	2.1580-2.8799i	2.1580-2.8799i

TABLE XI. Low-lying ($n \leq l$, with $l = j - 3/2$) spin-3/2 field quasinormal frequencies using the WKB and the AIM with $D = 5$ and $Q = M$.

Five dimensions				
l	n	WKB third order	WKB sixth order	AIM
0	0	0.7636-0.2260i	0.7748-0.2267i	0.7748-0.2266i
1	0	1.1542-0.2239i	1.1579-0.2242i	1.1578-0.2242i
1	1	1.0713-0.6900i	1.0828-0.6866i	1.0827-0.6866i
2	0	1.5404-0.2232i	1.5420-0.2233i	1.5420-0.2233i
2	1	1.4797-0.6787i	1.4853-0.6776i	1.4853-0.6776i
2	2	1.3701-1.1560i	1.3734-1.1563i	1.3734-1.1563i
3	0	1.9256-0.2229i	1.9264-0.2229i	1.9264-0.2229i
3	1	1.8779-0.6740i	1.8809-0.6735i	1.8809-0.6735i
3	2	1.7885-1.1394i	1.7906-1.1393i	1.7906-1.1393i
3	3	1.6656-1.6221i	1.6574-1.6323i	1.6574-1.6323i
4	0	2.3105-0.2227i	2.3110-0.2227i	2.3110-0.2227i
4	1	2.2713-0.6717i	2.2731-0.6714i	2.2731-0.6714i
4	2	2.1961-1.1305i	2.1975-1.1304i	2.1975-1.1304i
4	3	2.0903-1.6027i	2.0852-1.6076i	2.0852-1.6076i
4	4	1.9591-2.0886i	1.9383-2.1120i	1.9383-2.1120i
5	0	2.6953-0.2226i	2.6957-0.2226i	2.6957-0.2226i
5	1	2.6620-0.6703i	2.6631-0.6701i	2.6631-0.6701i
5	2	2.5973-1.1252i	2.5982-1.1252i	2.5982-1.1252i
5	3	2.5048-1.5905i	2.5014-1.5932i	2.5014-1.5932i
5	4	2.3884-2.0674i	2.3738-2.0806i	2.3738-2.0806i
5	5	2.2513-2.5556i	2.2176-2.5942i	2.2176-2.5942i

TABLE X. Low-lying ($n \leq l$, with $l = j - 3/2$) spin-3/2 field quasinormal frequencies using the WKB and the AIM with $D = 6$, 7 and $Q = 0.5$ M.

Six dimensions					Seven dimensions				
l	n	WKB third order	WKB sixth order	AIM	l	n	WKB third order	WKB sixth order	AIM
0	0	1.2225-0.3706i	1.2484-0.3817i	1.2484-0.3816i	0	0	1.6352-0.4888i	1.6769-0.5175i	1.6769-0.5175i
1	0	1.7034-0.3764i	1.7124-0.3790i	1.7130-0.3777i	1	0	2.1983-0.4993i	2.2147-0.5067i	2.2147-0.5067i
1	1	1.5222-1.1710i	1.5568-1.1692i	1.5568-1.1692i	1	1	1.8724-1.5650i	1.9497-1.5713i	1.9497-1.5713i
2	0	2.1698-0.3789i	2.1739-0.3794i	2.1739-0.3794i	2	0	2.7387-0.5037i	2.7474-0.5046i	2.7471-0.5046i
2	1	2.0344-1.1593i	2.0504-1.1572i	2.0504-1.1572i	2	1	2.4972-1.5452i	2.5363-1.5413i	2.5363-1.5413i
2	2	1.7938-1.9903i	1.8052-1.9976i	1.8052-1.9976i	2	2	2.0540-2.6772i	2.0923-2.6761i	2.0923-2.6761i
3	0	2.6314-0.3803i	2.6335-0.3804i	2.6335-0.3804i	3	0	3.2711-0.5057i	3.2757-0.5056i	3.2757-0.5056i
3	1	2.5230-1.1553i	2.5313-1.1538i	2.5313-1.1538i	3	1	3.0786-1.5383i	3.1001-1.5339i	3.1001-1.5339i
3	2	2.3230-1.9653i	2.3273-1.9684i	2.3273-1.9684i	3	2	2.7136-2.6303i	2.7337-2.6236i	2.7337-2.6236i
3	3	2.0525-2.8150i	2.0259-2.8605i	2.0259-2.8605i	3	3	2.2117-3.8007i	2.1600-3.8499i	2.1600-3.8499i
4	0	3.0911-0.3813i	3.0923-0.3813i	3.0923-0.3813i	4	0	3.8003-0.5069i	3.8028-0.5067i	3.8028-0.5067i
4	1	3.0003-1.1538i	3.0051-1.1529i	3.0051-1.1529i	4	1	3.6393-1.5354i	3.6518-1.5324i	3.6518-1.5324i
4	2	2.8293-1.9521i	2.8307-1.9537i	2.8307-1.9537i	4	2	3.3291-2.6061i	3.3398-2.6008i	3.3398-2.6008i
4	3	2.5928-2.7828i	2.5712-2.8088i	2.5712-2.8088i	4	3	2.8920-3.7372i	2.8530-3.7610i	2.8530-3.7610i
4	4	2.3025-3.6437i	2.2336-3.7479i	2.2336-3.7479i	4	4	2.3523-4.9324i	2.1898-5.0856i	2.1898-5.0856i
5	0	3.5499-0.3819i	3.5506-0.3819i	3.5506-0.3819i	5	0	4.3278-0.5077i	4.3294-0.5076i	4.3294-0.5076i
5	1	3.4716-1.1532i	3.4746-1.1527i	3.4746-1.1527i	5	1	4.1890-1.5341i	4.1967-1.5323i	4.1967-1.5323i
5	2	3.3221-1.9444i	3.3224-1.9454i	3.3224-1.9454i	5	2	3.9188-2.5922i	3.9248-2.5888i	3.9248-2.5888i
5	3	3.1120-2.7621i	3.0951-2.7781i	3.0951-2.7781i	5	3	3.5322-3.6979i	3.5026-3.7110i	3.5026-3.7110i
5	4	2.8514-3.6067i	2.7965-3.6724i	2.7965-3.6724i	5	4	3.0476-4.8579i	2.9241-4.9499i	2.9241-4.9499i
5	5	2.5466-4.4755i	2.4344-4.6523i	2.4344-4.6523i	5	5	2.4801-6.0708i	2.1989-6.3684i	2.1989-6.3684i

TABLE XII. Low-lying ($n \leq l$, with $l = j - 3/2$) spin-3/2 field quasinormal frequencies using the WKB and the AIM with $D = 6, 7$ and $Q = M$.

Six dimensions					Seven dimensions				
l	n	WKB third order	WKB sixth order	AIM	l	n	WKB third order	WKB sixth order	AIM
0	0	1.1597-0.3598i	1.1816-0.3675i	1.1816-0.3674i	0	0	1.5619-0.4825i	1.5886-0.5104i	1.5886-0.5104i
1	0	1.6468-0.3575i	1.6557-0.3593i	1.6557-0.3593i	1	0	2.1226-0.4825i	2.1369-0.4882i	2.1369-0.4882i
1	1	1.4621-1.1141i	1.4941-1.1081i	1.4941-1.1081i	1	1	1.7977-1.5148i	1.8602-1.5197i	1.8602-1.5197i
2	0	2.1237-0.3565i	2.1282-0.3568i	2.1282-0.3568i	2	0	2.6667-0.4819i	2.6752-0.4824i	2.6752-0.4824i
2	1	1.9865-1.0905i	2.0037-1.0867i	2.0037-1.0867i	2	1	2.4248-1.4788i	2.4613-1.4728i	2.4613-1.4728i
2	2	1.7385-1.8755i	1.7499-1.8733i	1.7499-1.8733i	2	2	1.9778-2.5675i	2.0051-2.5593i	2.0051-2.5593i
3	0	2.5979-0.3559i	2.6003-0.3559i	2.6003-0.3559i	3	0	3.2055-0.4811i	3.2103-0.4809i	3.2103-0.4809i
3	1	2.4891-1.0802i	2.4990-1.0780i	2.4990-1.0780i	3	1	3.0132-1.4630i	3.0353-1.4574i	3.0353-1.4574i
3	2	2.2845-1.8379i	2.2927-1.8346i	2.2927-1.8346i	3	2	2.6446-2.5031i	2.6659-2.4884i	2.6659-2.4884i
3	3	2.0038-2.6373i	1.9791-2.6610i	1.9791-2.6610i	3	3	2.1348-3.6254i	2.0774-3.6483i	2.0774-3.6483i
4	0	3.0710-0.3555i	3.0725-0.3555i	3.0725-0.3555i	4	0	3.7422-0.4805i	3.7452-0.4803i	3.7452-0.4803i
4	1	2.9808-1.0748i	2.9869-1.0736i	2.9869-1.0736i	4	1	3.5823-1.4546i	3.5963-1.4508i	3.5963-1.4508i
4	2	2.8077-1.8174i	2.8134-1.8150i	2.8134-1.8150i	4	2	3.2705-2.4682i	3.2860-2.4568i	3.2860-2.4568i
4	3	2.5640-2.5920i	2.5492-2.6021i	2.5492-2.6021i	4	3	2.8265-3.5433i	2.7943-3.5431i	2.7943-3.5431i
4	4	2.2621-3.4002i	2.1950-3.4647i	2.1950-3.4647i	4	4	2.2767-4.6878i	2.1118-4.7819i	2.1118-4.7819i
5	0	3.5438-0.3552i	3.5448-0.3552i	3.5448-0.3552i	5	0	4.2782-0.4800i	4.2801-0.4799i	4.2801-0.4799i
5	1	3.4667-1.0716i	3.4707-1.0709i	3.4707-1.0709i	5	1	4.1410-1.4495i	4.1502-1.4471i	4.1502-1.4471i
5	2	3.3169-1.8051i	3.3209-1.8036i	3.3209-1.8036i	5	2	3.8711-2.4475i	3.8824-2.4397i	3.8824-2.4397i
5	3	3.1025-2.5636i	3.0932-2.5684i	3.0932-2.5684i	5	3	3.4802-3.4920i	3.4614-3.4866i	3.4614-3.4866i
5	4	2.8329-3.3502i	2.7864-3.3853i	2.7864-3.3853i	5	4	2.9864-4.5939i	2.8744-4.6353i	2.8744-4.6353i
5	5	2.5157-4.1645i	2.4036-4.2794i	2.4036-4.2794i	5	5	2.4079-5.7543i	2.1250-5.9489i	2.1250-5.9489i

$$W|_{j \rightarrow \infty} \approx \frac{j\sqrt{f}}{r}, \quad V|_{j \rightarrow \infty} \approx \frac{j^2 f}{r^2}, \quad (4.11)$$

where f is given by Eq. (4.1). The corresponding r_{\max} , which represents $V(r_{\max})$ as the maximum of the effective potential is

$$r_{\max}^{(D-3)} = \frac{4(D-2)(r_+ r_-)^{(D-3)}}{(D-1)(r_+^{(D-3)} + r_-^{(D-3)}) - [(D-1)^2(r_+^{(D-3)} + r_-^{(D-3)})^2 - 16(D-2)(r_+ r_-)^{(D-3)}]^{1/2}}. \quad (4.12)$$

Then

$$V_0 = \frac{j^2}{r_{\max}^2} \left(\frac{D-3}{D-2} \right) \left(1 - \frac{1}{2}\eta \right), \quad (4.13)$$

$$V_0'' = -\frac{V_0^2}{j^2} (D-3)[4 - (D-1)\eta], \quad (4.14)$$

where $\eta \equiv (r_+^{(D-3)} + r_-^{(D-3)})/r_{\max}^{(D-3)}$. The analytic form of the QNMs in the large angular limit is

$$\omega \approx \left(\frac{D-3}{D-2} \right)^{1/2} \frac{(1 - \frac{1}{2}\eta)^{1/2}}{r_{\max}} \left\{ j - i \left(n + \frac{1}{2} \right) \right. \\ \left. \times \left[2(D-3) \left(1 - \frac{D-1}{4}\eta \right) \right]^{1/2} \right\}. \quad (4.15)$$

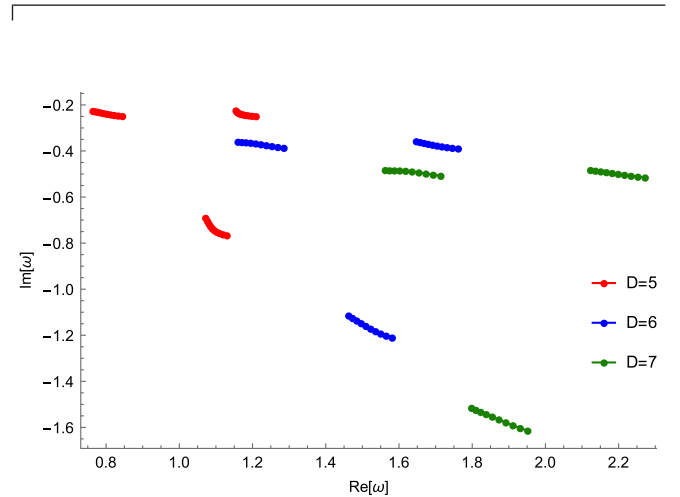


FIG. 4. The change of the first three QNM frequencies when Q increases from 0 to 1.

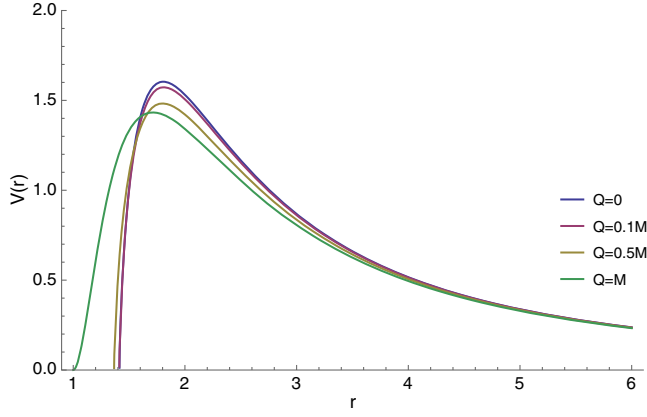


FIG. 5. The TT effective potential of $D = 5$ and $j = 5/2$ for $Q = 0$ to $Q = 1$.

Lastly, we have to note that this analytic form is a general one for fermionic fields in Schwarzschild ($Q = 0$) and Reissner-Nordström ($Q \leq M$) spacetimes.

V. ABSORPTION PROBABILITIES

In this section we present the absorption probabilities associated with our spin-3/2 fields near a Reissner-Nordström black hole. We use the same approach as in

Ref. [4], and as such only present the analysis of the results here, and refer the reader to Ref. [4] for the implementation of the method.

A. Non-TT eigenmodes related

In Fig. 6 we see that for a specific Q and D , the behavior of the absorption probability shifts from lower energy to higher energy as j increases, and this trend is similar to the Schwarzschild case. For fixed j and Q , we can compare the scale of each subplot and realize a lower energy to higher energy shift as D increase. For a fixed j and D , the absorption probability also shifts from left to right as Q increases. This is due to the maximum value of the corresponding potential increasing as Q increases, as shown in Fig. 3 for the case of $D = 5$, $j = 5/2$. An exception is in $j = 3/2$, $D = 7$ case, where the curve shifts to the left instead. This is because the maximum value of the potential decreases instead of increasing as Q is increased. Moreover, we have left out the absorption probability in the case of $j = 3/2$, $D = 7$, and $Q = 1$. We could not obtain a satisfactory curve for this case and believe this is due to the fact that the effective potential has two local maxima rather than one, thus rendering the WKB approximation inapplicable.

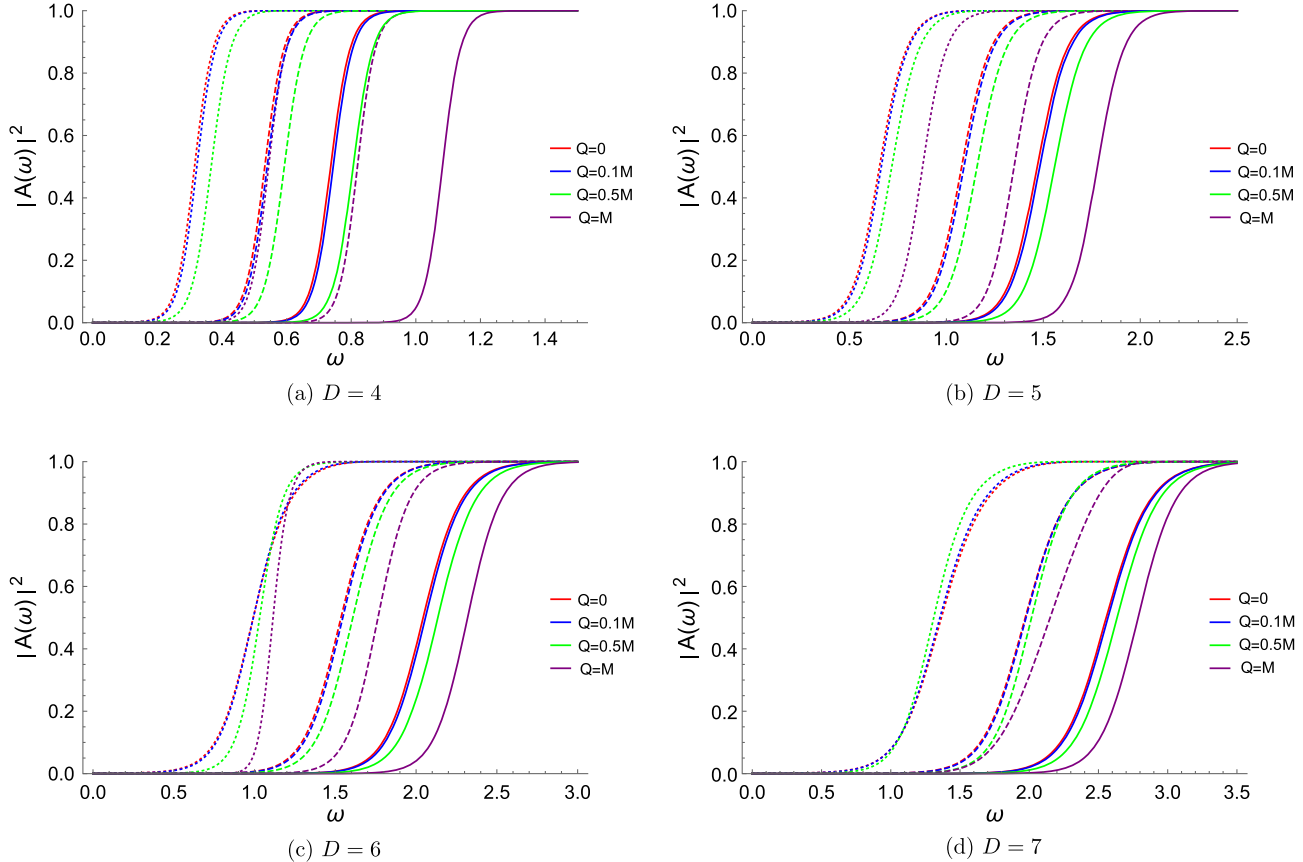


FIG. 6. Spin-3/2 field absorption probabilities for various dimensions and $j = 3/2$ (dotted), $j = 5/2$ (dashed) and $j = 7/2$ (solid).

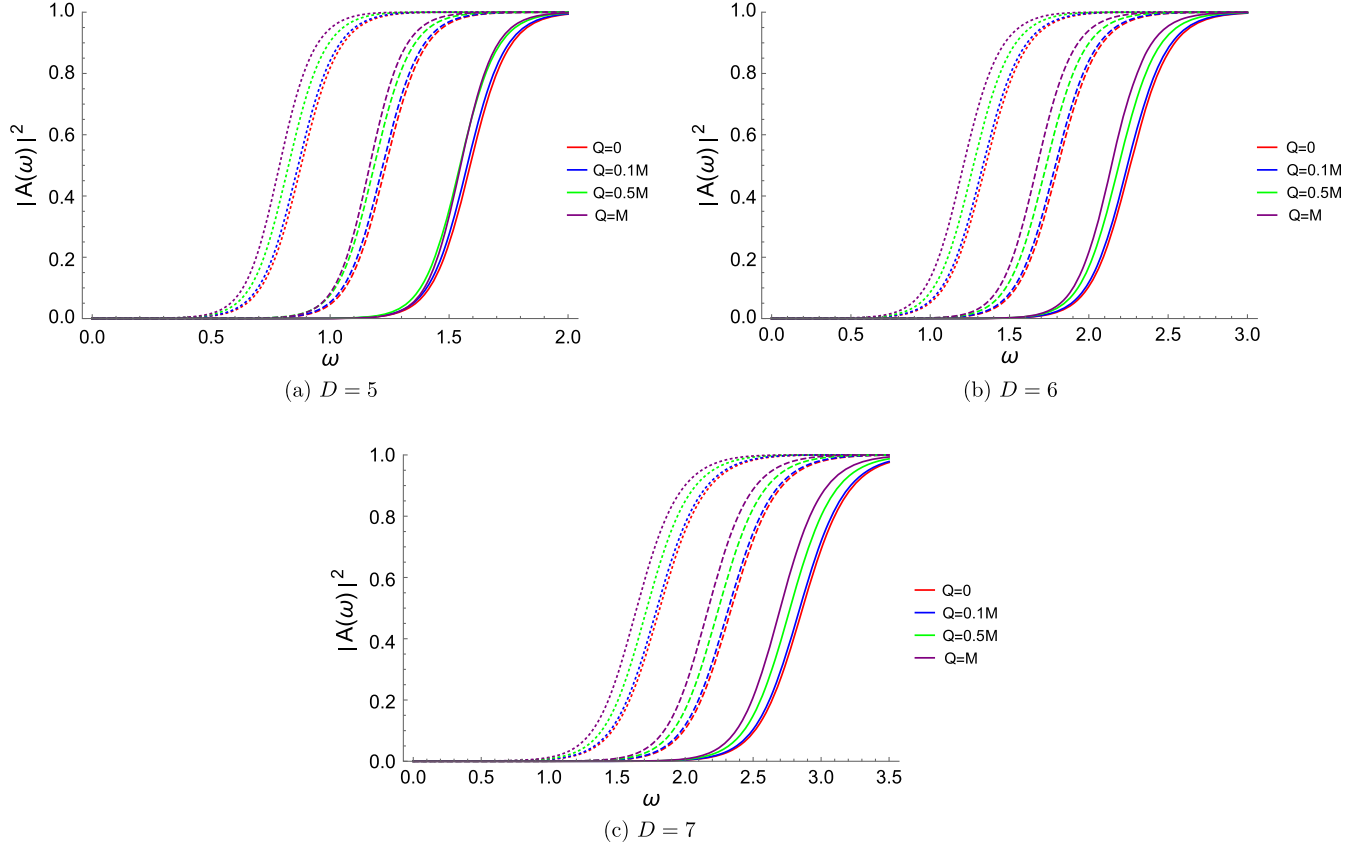


FIG. 7. Spin-3/2 field absorption probabilities with various dimensions and $j = 3/2$ (dotted), $j = 5/2$ (dashed) and $j = 7/2$ (solid).

B. TT eigenmodes related

The absorption probabilities associated with the TT eigenmodes are present in Fig. 7. It is clear that the absorption probabilities shift from lower energy to higher energy when we increase j (with fixed Q and D), and when we increase D (with fixed Q and j). However, when Q is increased with fixed D and j , the absorption probabilities shift from higher energy to lower energy. This is due to the maximum value of effective potential decreasing when Q increases, as shown in Fig. 5 for the typical case of $D = 5$, $j = 5/2$.

VI. DISCUSSION AND CONCLUSION

In this paper we continue with our previous consideration of spin-3/2 fields in higher dimensional spherically symmetry black hole spacetimes [3,4]. The first difference we encounter is the modification of the covariant derivative to the supercovariant derivative for spacetimes with a nonvanishing Ricci tensor, in which Reissner-Nordström black hole spacetime was the example studied here. This modification is necessary to maintain the supersymmetric gauge symmetry. We have not shown it explicitly in this paper, but the same procedure can also be applied to asymptotic nonflat cases, like black holes in de Sitter and anti-de Sitter spaces.

Our main results on the QNM frequencies and the absorption probabilities of the spin-3/2 fields for both non-TT eigenmodes and TT eigenmodes are given in Secs. IV and V, respectively. First we looked at the non-TT modes, where we found that when the charge of the black hole Q is increased from 0 to M the maximum value of the effective potential increases, while the peak of the potential becomes sharper (Fig. 3 is a typical example). The result of this on the quasinormal frequencies is that both the real part and the magnitude of the imaginary part increase. For the absorption probability the curve shifts to higher energy when Q is increased. However, this trend is reversed from the $j = 3/2$ and $D = 7$ case upwards, such that the maximum value of the potential instead decreases as Q is increased. For higher dimensions, more and more modes would have this behavior.

For the TT modes, the situation seems to be simpler. First we need to mention that the effective potential in this case is not the same as the one for Dirac fields in the same spacetime; this is due to the extra terms present in the supercovariant derivative. A typical example of the change of the potential with changing Q is given in Fig. 5. We can see that when Q is increased, the maximum value of the potential decreases and the peak broadens. Hence, the corresponding real part of the quasinormal frequency decreases, and so too the magnitude of the imaginary part.

For the absorption probability the curve then shifts to lower energies as Q is increased. This is opposite to the trend observed for the non-TT cases when the dimension is $D < 7$.

We have found that for higher dimensions, and especially for the charge Q near the extremal value, the effective potential develops another maximum. We believe that this is also a property of the potentials in high enough dimensions. The shape of the potential becomes more complicated due to the appearance of more maxima and minima. This poses difficulties to the WKB approximations and the AIM we used to evaluate the QNMs, as well as the absorption probabilities. This problem is more prominent for larger values of Q , especially for the extremal cases.

Since our method is applicable to spherically symmetric spacetimes, the immediate applications would be to consider spin-3/2 fields for Schwarzschild and Reissner-Nordström black holes in de Sitter and anti-de Sitter spaces. Charged black holes in anti-de Sitter spaces are particularly interesting because of their relevance to the

ground state of supergravity. With these studies we may have a general discussion of fermionic QNMs in spherically symmetric spacetimes, such as those that were done for bosonic fields; see Refs. [12,13]. We are also interested in working out the absorption cross sections in our subsequent works. To do that we need to find the degeneracies of the eigenspinor vectors on the N sphere. One should be able to do that by following the method of Camporesi and Higuchi developed for Dirac spinors [14].

ACKNOWLEDGMENTS

A. S. C. and G. E. H. are supported in part by the National Research Foundation of South Africa. C. H. C. and H. T. C. are supported in part by the Ministry of Science and Technology, Taiwan, Republic of China under Grant No. 105-2112-M-032-004. H. T. C. is also supported in part by the National Center for Theoretical Sciences (NCTS). C. H. C. is also supported in part by Taipei Gravitational Wave Group, National Taiwan Normal University.

-
- [1] A. Das and D. Z. Freedman, *Nucl. Phys.* **B114**, 271 (1976).
 - [2] M. T. Grisaru, H. N. Pendelton, and P. van Nieuwenhuizen, *Phys. Rev. D* **15**, 996 (1977).
 - [3] C. H. Chen, H. T. Cho, A. S. Cornell, G. Harmsen, and W. Naylor, *Chin. J. Phys. (Taipei)* **53**, 110101 (2015).
 - [4] C. H. Chen, H. T. Cho, A. S. Cornell, and G. Harmsen, *Phys. Rev. D* **94**, 044052 (2016).
 - [5] R. A. Konoplya and A. Zhidenko, *Rev. Mod. Phys.* **83**, 793 (2011).
 - [6] R. A. Konoplya, *Phys. Rev. D* **68**, 024018 (2003).
 - [7] H. T. Cho, A. S. Cornell, J. Doukas, T.-R. Huang, and W. Naylor, *Adv. Theor. Math. Phys.* **2012**, 281705 (2012).
 - [8] J. T. Liu, L. A. P. Zayas, and Z. Yang, *J. High Energy Phys.* **02** (2014) 095.
 - [9] H. Kodama and A. Ishibashi, *Prog. Theor. Phys.* **111**, 29 (2004).
 - [10] H. T. Cho, A. S. Cornell, J. Doukas, and W. Naylor, *Phys. Rev. D* **75**, 104005 (2007).
 - [11] S. Iyer and C. M. Will, *Phys. Rev. D* **35**, 3621 (1987).
 - [12] V. Cardoso, J. P. S. Lemos, and S. Yoshida, *J. High Energy Phys.* **12** (2003) 041.
 - [13] V. Cardoso, J. P. S. Lemos, and S. Yoshida, *Phys. Rev. D* **69**, 044004 (2004).
 - [14] R. Camporesi and A. Higuchi, *J. Geom. Phys.* **20**, 1 (1996).